

ARTICLE

Surface Temperature Variability in Urban Street Canyons in a Tropical Climate

Letzai Ruiz-Valero * , Virginia Flores-Sasso , Victor W. Bohorquez-Lopez , Orisell Medina-Lagrange 

School of Civil and Environmental Engineering, Pontificia Universidad Católica Madre y Maestra (PUCMM), Abraham Lincoln esq. Rómulo Betancourt, 10109, Santo Domingo, Dominican Republic

ABSTRACT

Materials used in building envelopes and urban areas contribute significantly to the urban heat island (UHI). In this context, this paper presents a study utilizing infrared thermography (IRT) to assess urban streets and building surface materials in the coastal city of Bayahibe, Dominican Republic. Measurements were conducted *in situ* in six urban street canyons (Sections A–F) during the warmest and coldest weather conditions. A FLIR T420 thermal camera, FLIR Tools+ software, and the emissivity values of common building materials in Bayahibe were used to determine surface temperatures under sunlit and shaded conditions. The findings show that sunlit surfaces of urban elements generally exhibited higher surface temperatures compared to their shaded counterparts in both warm and cold periods. Metal surfaces displayed the most significant surface temperature differences between sunlit and shaded areas. Additionally, light-colored block walls presented lower surface temperatures than medium and dark-colored ones. This research provides insights into the urban microclimate of Bayahibe under different meteorological conditions. It supports the development of strategies to mitigate the UHI effect and enhance pedestrian thermal comfort in tropical and coastal cities by emphasizing the importance of shading elements and light-colored surfaces. The findings can inform specific interventions and policies for creating more sustainable and climate-resilient urban environments in the Caribbean region.

Keywords: Urban Streets; Surface Materials; Thermal Images; Infrared Thermography; Tropical Climate; Caribbean City

*CORRESPONDING AUTHOR:

Letzai Ruiz-Valero, School of Civil and Environmental Engineering, Pontificia Universidad Católica Madre y Maestra (PUCMM), Abraham Lincoln esq. Rómulo Betancourt, 10109, Santo Domingo, Dominican Republic; Email: letzairuiz@pucmm.edu.do

ARTICLE INFO

Received: 30 July 2025 | Revised: 10 August 2025 | Accepted: 14 August 2025 | Published Online: 27 August 2025

DOI: <https://doi.org/10.30564/jbms.v7i3.11398>

CITATION

Ruiz-Valero, L., Flores-Sasso, V., Bohorquez-Lopez, V.W., et al., 2025. Surface Temperature Variability in Urban Street Canyons in a Tropical Climate. *Journal of Building Material Science*. 7(3): 118–142. DOI: <https://doi.org/10.30564/jbms.v7i3.11398>

COPYRIGHT

Copyright © 2025 by the author(s). Published by Bilingual Publishing Group. This is an open access article under the Creative Commons Attribution-NonCommercial 4.0 International (CC BY-NC 4.0) License (<https://creativecommons.org/licenses/by-nc/4.0/>).

1. Introduction

Urban areas in tropical regions are increasingly impacted by rising temperatures and the urban heat island (UHI) effect, posing a significant threat to the health and well-being of urban populations worldwide ^[1]. In recent decades, heat stress has become an emerging threat in the Caribbean region for coral reefs, livestock, labor productivity, and human health, with these sectors being the most affected ^[2]. Projections indicate that 68% of the world's population will reside in urban areas by 2050; hence, understanding and mitigating UHI is critical for ensuring a sustainable and comfortable urban environment ^[3]. Rising temperatures and extreme weather events exacerbate heat stress in rapidly growing urban communities ^[4]. One of the main reasons for the UHI is the materials used for building envelopes and urban areas ^[5]. In public areas, paved surfaces contribute significantly to heat storage and release ^[6]. These surface temperature dynamics can be assessed using infrared thermography (IRT), a non-invasive thermal imaging technique, which serves as a tool for assessing the thermal performance of urban landscapes ^[7].

The possibilities offered by IRT application range from the inspection of a single building to the analysis of entire neighborhoods, allowing for the evaluation of various objectives (e.g., quality of building envelopes, preventive maintenance, UHI effect) ^[8,9]. By capturing surface temperature variations, IRT enables researchers and urban planners to identify heat contributors and mitigators within the built environment ^[10]. Within urban boundaries, thermal thresholds above the average surface temperature of 6 °C emerge as a key indicator of critical heat zones, useful for early warning systems during urban heat waves ^[11]. For this reason, this study applies IRT to characterize the thermal behavior of urban streets and building construction materials in a Caribbean city, providing data for decision making to inform heat mitigation, heat distribution patterns, and climate-resilient urban planning in tropical climates, contributing to the fulfillment of Sustainable Development Goals 11 and 13.

Using IRT to analyze how the thermal energy of urban surfaces varies during a diurnal cycle, Quattrochi and Ridd ^[12] determined that properties such as heat capacity, thermal conductivity, and soil moisture significantly influence

the amount of thermal energy emitted and its behavior between day and night. Dorer et al. ^[13] found that the urban microclimate is determined by local air velocity, temperature and humidity, solar irradiation and specular and diffuse reflections, the surface temperatures of buildings and ground, and the respective long-wave radiation exchange with the sky.

Research has been carried out worldwide to analyze the urban streets and surface materials by applying IRT, such as Klimenka et al. ^[6], which compared building façade surface temperatures from a simulated model and onsite thermal images in London, Canada. While Kawakubo et al. ^[14] analyzed the surface of urban roadway using thermal images obtained from a moving car to identify hotter and cooler areas in Tokyo, Japan. Rodrigues et al. ^[15] used aerial thermography and simulation tools to evaluate an urban canyon in the city of Huelva, Spain, analyzing thermal comfort in terms of predicted mean vote and predicted percentage of dissatisfied to create design recommendations to improve urban comfort. Also, Malcoti et al. ^[10] assessed the thermal properties of physical elements in residential streets in the city of Gurugram, India, using a thermal camera, with special emphasis on how impermeable surfaces affect the environment. Elmarakby et al. ^[1] studied the UHI effect in the Greater Cairo Region in Egypt, implementing various tools such as remote sensing, thermal images, and field air temperature monitors. Additionally, Rodríguez et al. ^[16] implemented aerial thermography in Huelva, Spain, to measure the radiant heat transfer in a pedestrian urban space during a summer day. Meanwhile, Garcia-Nevado et al. ^[17] used thermal images to analyze the cooling effect of urban textile shading in some streets of Cordoba, Spain. Lee et al. ^[18] assessed thermal characteristics of various physical elements on three major commercial streets in Seoul, Korea, applying IRT to improve pedestrian thermal comfort.

In tropical climates, some research has been conducted, such as Martinet al. ^[4], who developed an infrared observatory in Singapore to analyze the contributors to the UHI and its mitigators at the neighborhood level, as well as Ramani et al. ^[9], who used the same observatory to conduct neighborhood-scale thermal imaging research to identify hot and cold spots in urban areas of Singapore. Also, in Indonesia, Febrita and Hartono ^[19] analyzed the

thermal characteristics of various urban street surface materials using IRT in two main commercial streets in Banjarbaru. Meanwhile, Binarti et al. ^[20] combined techniques to identify the contribution of vertical and horizontal surface materials to the UHI using an infrared camera and satellite thermal images in two street canyons in the city of Yogyakarta.

Although several studies have explored the thermal behavior of urban streets and building surface materials in different climates, there is a need for research focused on the specific characteristics of Caribbean cities. This paper addresses this gap by presenting a study that utilizes IRT to assess urban streets and building surface materials in a Caribbean city during the warmest and coldest weather conditions.

The structure of the paper is organized as follows: Section 2 outlines the case study comprising the location, climate conditions, and description of the study area. Section 3 comprises the methodology used to conduct thermal images. Section 4 examines the results and discussion or-

ganized by urban street canyons. Finally, Section 5 presents the conclusions and further research.

2. Case Study

2.1. Location

The case study is Bayahibe, an original fishing village founded in 1874 in the province of La Altagracia, Dominican Republic, on the southern coast of the Caribbean Sea ^[21], which acquired the category of section in 1939, belonging to the community of Higüey ^[22]. Located at an elevation of 62.4 meters (204.72 feet) above sea level, at 18°22'00" N 68°50'00" W, the UTM position is zone 19Q E: 526283.75 N: 2025486.58 ^[23]. Bayahibe borders the Parque Nacional del Este Cotubanama (Cotubanama Eastern National Park), and seven springs are in the area ^[24]. **Figure 1** shows on the left side the location of the Dominican Republic and Bayahibe, while on the right side is a bird's eye view of the urban area of Bayahibe.



Figure 1. Location of Bayahibe and a bird's eye view of the urban area of Bayahibe ^[25].

2.2. Climate Conditions

According to the Köppen-Geiger climate classification, Bayahibe has a tropical savannah climate (Aw), characterized by warm temperatures throughout the year with high humidity ^[26]. Average annual temperatures hover around 27 °C, with daytime highs ranging from 30 °C in January to 33 °C in August. Nighttime temperatures typi-

cally vary from 20 °C in January to 23 °C in July ^[27]. The region experiences a pronounced wet season from May to November, during which rainfall is more frequent and intense. Conversely, the dry season spans from December to April, offering sunnier and drier conditions ^[28]. The average annual rainfall in Bayahibe is approximately 54.23 mm, receiving an average of 152.72 mm of rain ^[29]. **Figure 2** presents the weather conditions in Bayahibe.

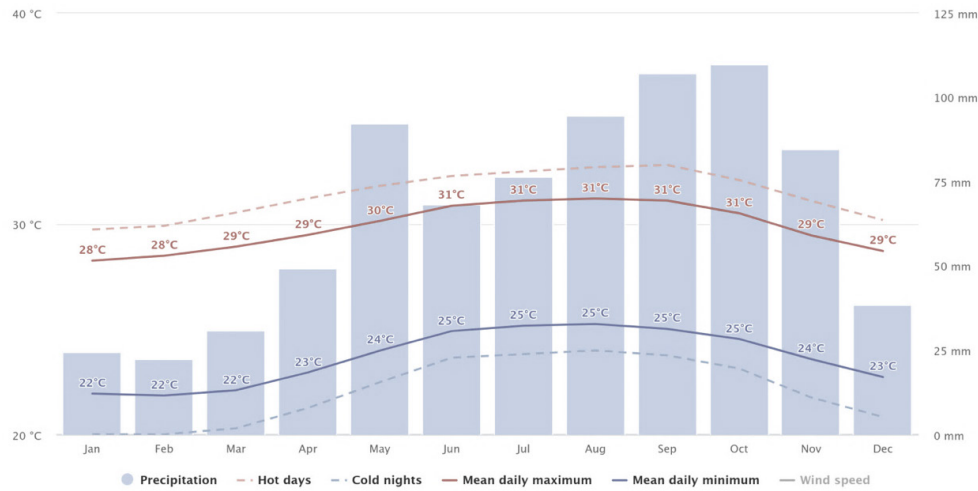


Figure 2. Weather conditions in Bayahibe [27].

2.3. Description of the Study Area

According to the X National Census of Population and Housing of 2022, the tourist municipality of Bayahibe has a population of 5618 inhabitants and a territorial extension of 218.40 km², which results in a population density of 26 inhabitants/km². However, the urban nucleus of Bayahibe, which includes the historical center and a small contiguous area of growth, is 0.531 km², with an estimated population to date of 939 inhabitants, which significantly raises the population density to 1768 inhabitants/km² [30]. For this reason, the population density of Bayahibe varies significantly depending on the area being analyzed. Today, the growth of tourism, becoming one of the main engines of its evolution, is currently receiving about one million visitors a year who leave from its ports to visit Saona Island. As of February 2025, hotels in the area had an effective occupancy rate of 90.1% [23].

Bayahibe began as a temporary settlement of fishermen in the late 19th century, who gradually settled in the place informally with their families, building very simple huts, thus staying permanently in the area [22]. The settlement never had an orderly or official city plan since all the inhabitants stayed informally. The settlement was always unpaved (**Figure 3**) until 2016, when the authority placed concrete pavers on some streets in the oldest part of the city [21]. In 2023, some streets were paved with asphalt and concrete. It is important to note that from the beginning, in Bayahibe all the houses were made of wood with a Cana palm leaf roof. However, with the construction of a highway in 1977 and the increase of tourism [21], some buildings began to change their construction material, replacing the Cana roof with zinc sheeting, wooden walls with cement blocks, and wood windows for glass windows to name a few of the most significant changes.



Figure 3. Unpaved streets and wooden houses in Bayahibe, 1998 [31].

The old area of Bayahibe, which we have called the historic center, has no planned urban design because it emerged as an informal settlement that grew over time^[22]. Its streets are narrow, and most of them lack sidewalks. The blocks have different shapes and sizes. Within this perimeter, six urban canyons (Sections A–F) are used in this research, understanding “urban canyon” as the linear space

formed by two continuous rows of urban elements (e.g., buildings, vegetation, furniture) on both sides of a street or section, generating a “canyon” effect^[18]. The elements to be described in the urban canyon are orientation, height, and height/width (h/w) ratio, materiality, and vegetation. **Figure 4** shows the urban canyons (Sections A–F) and the IRT image capture points.

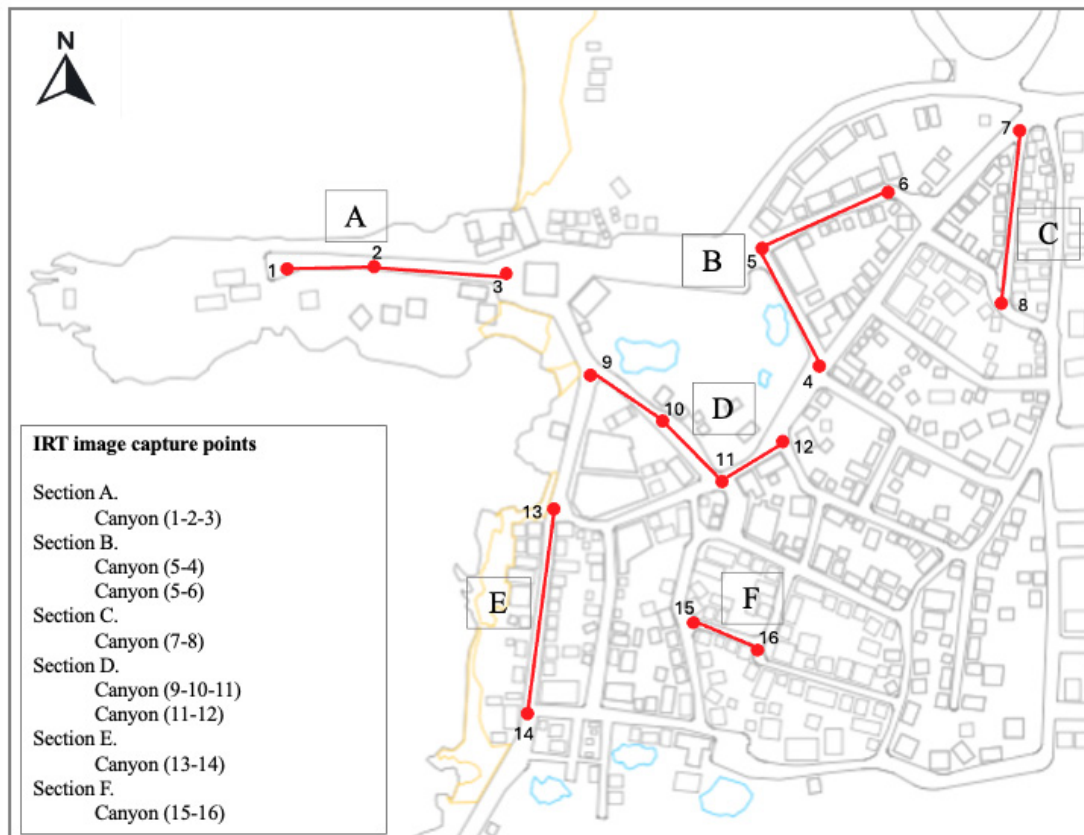


Figure 4. Urban canyons and IRT images capture points.

Section A contains Canyon (1–2–3). It is oriented West-East (W-E), formed by a parking lot and a few buildings on the South side, with an average height of 3.25 m. On the West side, there is only vegetation and sea, resulting in an h/w ratio of approximately 3:5, generating shadows on the pavement. The length of the canyon is (L – length / W – width) L: 123.70 m (405.83 ft) and W: 5.15 m (16.90 ft). The facades are of timber with zinc sheeting. The area has vegetation on both sides, and the ground is covered with concrete pavers, and the parking lot with asphalt.

Section B contains two canyons. Canyon (5-6) is oriented West-East (W-E), formed by 13 buildings of different

heights and shapes, seven of them on the South side and six on the North side, with a maximum height of 9.40 m and a minimum height of 2.85 m. The length of the canyon (5-6) is L: 72.52m (237.91ft) and W: 5.25m (17.24 ft). The material of the facades is timber with zinc sheeting. The canyon (5-4) is oriented North-South (N-S), the length is 68.74 m (225.53 ft) and width is 6.50 m (21.33 ft). On the West side, there is a green area with natural spring water, and it is not built, generating shadows on the pavement, but on the East side, there are three concrete buildings, with 3 different heights. In both canyons, the pavement is asphalt.

Section C, Canyon (7-8). It is oriented North-South

(N-S), formed by 17 buildings of different heights and shapes, six on the West side and eleven on the East side, with 3-level buildings, with a maximum height of 8.90 m and a minimum height of 2.70 m. The length of the canyon (7-8) is L: 85.90 m (281.81 ft) and W: 5.25m (17.24 ft). All buildings are concrete except one, which is wood with a zinc roof, and the facades have balconies. The street pavement is concrete.

Section D contains two canyons. Canyon (9-10-11) is oriented Northwest-Southeast (NW-SE), formed by six buildings, four on the North side and two on the other in the green area. This canyon has two fences with a height of 1.65 m. The length of the canyons is L: 82.47 m (270.57 ft) and W: 4.08 m (13.38 ft). The Canyon (11-12) is oriented Southwest-East (SW-E). The length of the canyons is L: 24.22 m (79.45 ft) and W: 6.29 m (20.64 ft). In this canyon, the ground is covered with concrete pavers.

Section E, Canyon (13-14), oriented North-South (N-S). The length of the canyons is L: 110.42 m (362.28 ft) and W: 6.80 m (22.31 ft). In this canyon, the ground is

covered with Concrete Pavers. All the buildings in this canyon are made of concrete blocks, and one is made of wood. The facades have balconies and there are two-story buildings that are up to 6.10 m in height. In this canyon, there are 21 buildings, with 11 on the east side and about 10 on the west side.

Section F, Canyon (15-16). It is a narrow canyon, oriented North-South (N-S). The length of the canyons is L: 37.51 m (123.06 ft) and W: 5.62 m (18.44 ft). In this canyon, there are 7 buildings, 4 are on the South side and 3 on the North side. The buildings are at one level, except one, which is two levels. They are predominantly built with concrete blocks, although there are also some wooden buildings.

Figure 5 shows the six urban street canyons (Sections A–F) studied, and the different points where thermal images were taken (e.g., 1-2: point 1 facing point 2, 2-1: point 2 facing point 1). Meanwhile, urban street canyon characteristics identified in each of the sections analyzed are provided in **Table 1**.

Table 1. Characteristics of the urban street canyons.

Street Canyon Scenario	Length the Canyon (L -Length) (W -Width)	Street Canyon Orientation	Urban Surfaces Material	H/W Aspect Ratio
Section A Canyon (1-2-3)	L: 123.70 m (405.83 ft) W: 5.15 m (16.90 ft)	West-East (W-E)	Asphalt road, concrete pavers, polished cement floor, zinc roof, concrete block wall, metal fence	1:1 Asymmetric
Section B Canyon (5-6)	L: 72.52m (237.91ft) W: 5.25m (17.24 ft)	West-East (W-E)	Asphalt road, concrete pavers, concrete sidewalk, block walls, concrete eaves, glass door, glass window	1:1 Asymmetric
Canyon (5-4)	L: 68.74 m (225.53 ft) W: 6.50m (21.33 ft)	North-South (N-S)	Asphalt road, concrete block wall, glass window	2:1 Asymmetric
Section C Canyon (7-8)	L: 85.90 m (281.81 ft) W: 5.25 m (17.24 ft)	North-South (N-S)	Asphalt road, block walls, glass window	2:1 Asymmetric
Section D Canyon (9-10-11)	L: 82.47 m (270.57 ft) W: 4.08 m (13.38 ft)	Northwest-Southeast (NW-SE)	Asphalt road, block walls, glass window	1:1 Asymmetric
Canyon (11-12)	L: 24.22 m (79.45 ft) W: 6.29 m (20.64 ft)	Southwest-East (SW-E)	Concrete pavers, concrete sidewalk, concrete block, wood wall, glass window, metal roof, stone fence	1:1 Asymmetric
Section E Canyon (13-14)	L: 110.42 m (362.28 ft) W: 6.80 m (22.31 ft)	North-South (N-S)	Concrete pavers, concrete sidewalk, concrete block wall, glass window	2:1 Asymmetric
Section F Canyon (15-16)	L: 37.51 m (123.06 ft) W: 5.62 m (18.44 ft)	North-South (N-S)	Asphalt road, concrete block wall, metal roof, tile roof	2:1 Asymmetric

Note: Asymmetric canyon, the buildings that make the canyon have significant height differences.



Figure 5. Urban street canyons assessed.

3. Materials and Methods

IRT was applied *in situ* to conduct the assessment of urban streets and building surface materials in Bayahibe. Six urban canyons were selected, representing different characteristics present in Bayahibe, such as a canyon located in front of the coast, a canyon with vegetation, a canyon with cost on both sides, an interior canyon with one-story buildings, and an interior canyon with mixed one- and two-story buildings. **Figure 4** shows the location of the six urban street canyons (A–F) assessed, and each point where thermal images were taken. The on-site measurements were conducted in two phases, during the warmest (August 16, 2024) and coldest (January 04, 2025) periods to carry out comparisons. The weather conditions on both days were sunny with an average air temperature of 31.6 °C and 25.5 °C, and relative humidity of 70% and 75%, respectively.

Thermal images were taken on each street canon using the infrared camera FLIR SYSTEMS model T420, FOL 18mm lens, and 240 × 320 pixels IR resolution. The camera has a spectral range of 7.5 to 13 microns and a field of view (FOV) of 25° x 19°/0.4 meters and a spatial resolution (IFOV) of 1.36 milliradians. The thermal range was set at –20 °C to 120 °C. The camera used for this analysis meets the requirements of the UNE-EN 13187:1998 standard, and the research is based on passive thermography, which is when the temperature differences of a structure are generated under normal conditions ^[32].

To carry out the thermal images, the standard UNE-EN 13187: 1998 / ISO 6781: 1983 modified ^[33] was followed. To obtain a precise value of the measurements, the emissivity values of the most common construction materials found in Bayahibe (e.g., concrete: 0.95, mortar: 0.94, masonry: 0.94, glass: 0.92, asbestos: 0.96) ^[34] were considered. FLIR Tools+ software, version 6.4.18039.1003, was used to analyze the thermal images, adjusting some parameters (e.g., air temperature, relative humidity, reflected apparent temperature, distance, and emissivity), and placing points in specific areas to measure the surface temperature value in that spot. An iron color palette mode was selected, where the reference colors are yellow for the hottest temperature range and blue for the coldest temperature range.

To analyze the data and generate the graphs, the mini-

um and maximum surface temperatures of each material were identified in the analyzed periods (the warmest and coldest), considering the sunlit or shaded conditions to calculate the average.

4. Results and Discussion

This section provides a summary of the thermal characteristics analysis of urban street canyons assessed in Bayahibe and is organized according to each section. Thermal images, visual images, and surface temperatures of the materials at each point taken during the warmest (August) and coldest (January) periods are included. Depending on the time at which the thermal images were taken, the urban form and the typology of the buildings, some urban elements are only measured in sunlit or shaded conditions.



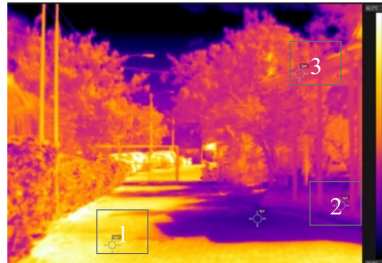
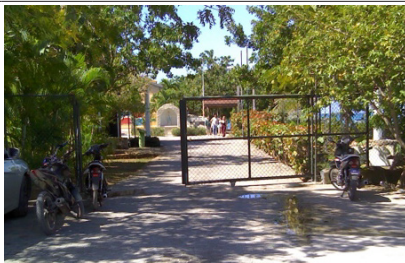
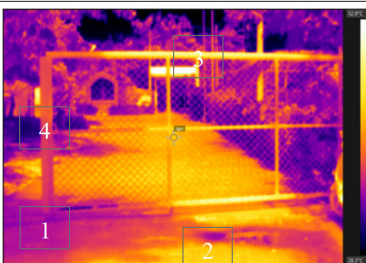
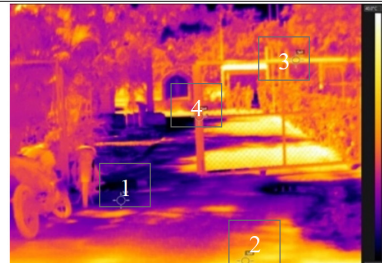
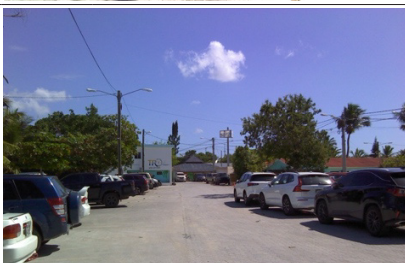





4.1. Section A

Table 2 shows the surface temperatures of the urban street elements and building materials evaluated in section A, based on the three thermal image points. The urban elements and building materials analyzed in this canyon are asphalt, concrete pavers, polished cement floor, asbestos roofing, block wall, metal eaves, metal fence, metal car surface, and tree surface.

Figure 6(A) presents surface temperatures during the warmest period in sunlit and shaded conditions. Most of the materials were studied in sunlit conditions, except for the polished cement floor, which was only analyzed in shaded conditions. On the other hand, only three materials were evaluated under shaded conditions. The metal car surface had the highest average surface temperature under sunlit conditions with 50.5 °C, while the lowest average surface temperature was for the light-colored block wall with 31.3 °C. Asbestos roofing, asphalt road, concrete pavers, and metal fence have surface temperatures above 40 °C. Similar results were presented in some studies conducted in Egypt and India, where the metal car was the most critical urban form subjected to massive heat storage from field measurements ^[1], and the light-colored buildings presented the lower surface temperature ^[10]. Comparing the average differences in surface temperatures between the metal fence in sunlit and shaded areas shows a difference of 9.6 °C, and the concrete pavers of 2.95 °C. This same

pattern is repeated during the coldest period [Figure 6(B)], but all average surface temperatures of the urban elements during sunlit conditions are below 40 °C. In this case, the average differences in surface temperatures between the concrete pavers in sunlit and shaded areas present a difference of 12.7 °C, and the metal fence of 5.6 °C.

Table 2. Surface temperatures of the street elements and building materials in section A.

	Visual Image	Thermal Image Aug.	Thermal Image Jan.	
1-2				
2-1				
2-3				
3-2				
	Spot	Surface	Temperature (°C) Aug.	Temperature (°C) Jan.
1-2	1	Concrete pavers sunlit	40.8	38.5
	2	Polished cement floor shaded	35.4	27.1
	3	Metal eaves sunlit	35.3	30.5
2-1	1	Concrete pavers shaded	35.8	26.0
	2	Concrete pavers sunlit	43.9	34.9
	3	Metal fence sunlit	47.9	36.9
	4	Metal fence shaded	38.3	31.3
2-3	1	Asphalt road sunlit	43.9	38.0
	2	Light-colored block wall sunlit	31.3	27.2
	3	Asbestos roofing sunlit	45.0	39.7
	4	Metal car surface sunlit	46.4	35.2
3-2	1	Concrete pavers sunlit	43.0	42.4
	2	Metal car surface sunlit	54.5	44.4
	3	Tree surface	32.9	30.9

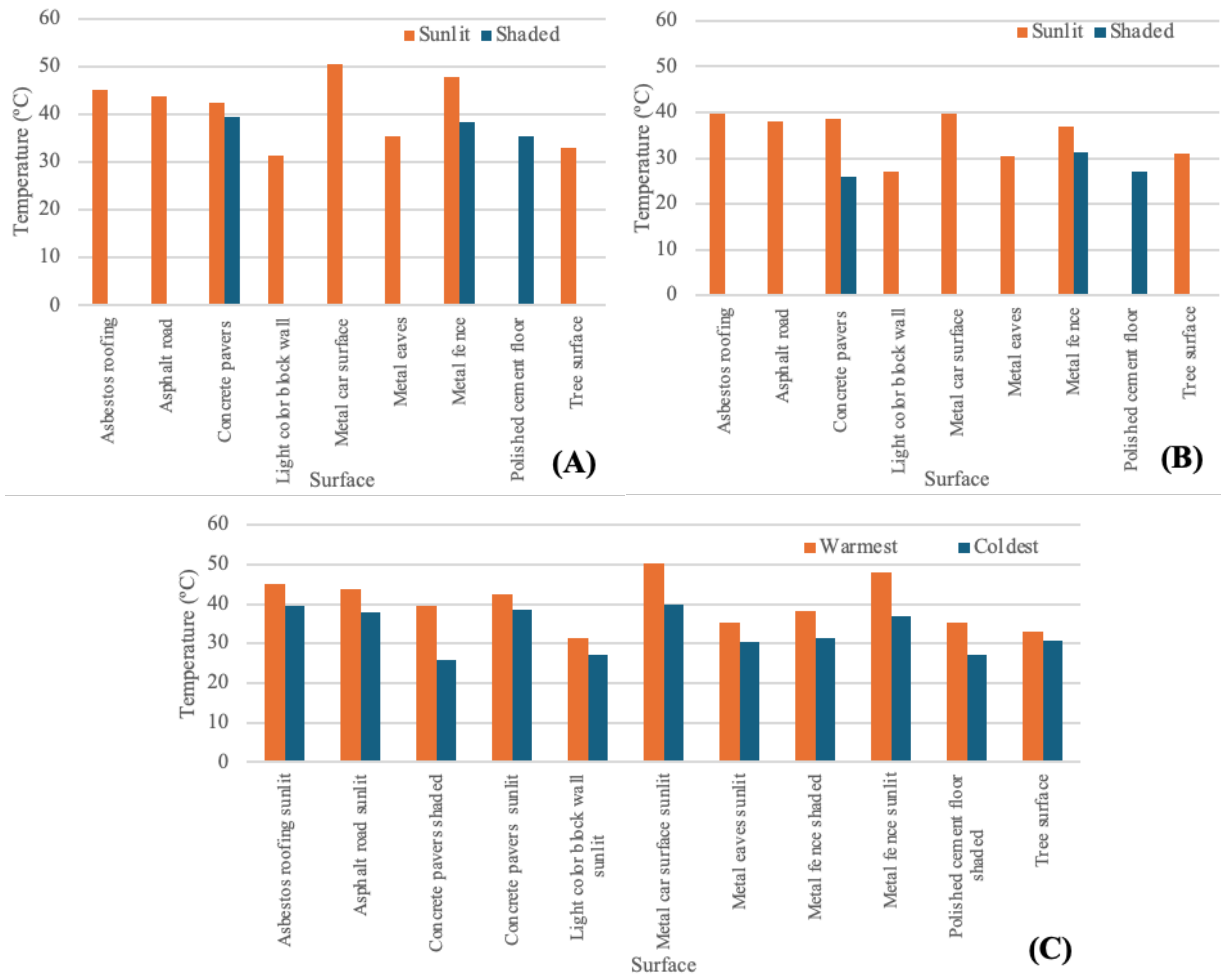


Figure 6. Surface temperature of the urban elements and building materials in Section A, (A) warmest period with sunlit and shaded, (B) coldest period with sunlit and shaded, and (C) both periods warmest-coldest.

Overall, this behavior is due to the urban element and building materials surfaces exposed to direct sunlight generally reach higher temperatures compared to those in shaded conditions. The intensity of sunlight and the angle at which it strikes the element surface affect the amount of heat absorbed. Similar results were presented in a study where the urban and building materials strongly influenced the occurrence of UHI in both the horizontal and vertical aspects, impacting the temperature of the urban form ^[1].


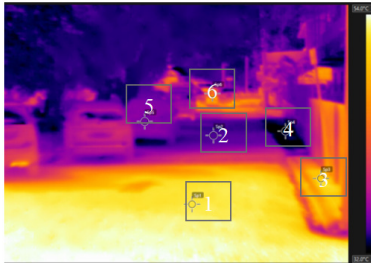










Analyzing the average surface temperature between the warmest and coldest periods, all urban elements and building materials reported higher average surface temperatures during the warmest period compared to the average surface temperatures of the coldest period [Figure 6(C)]. The largest average surface temperature difference occurs in the concrete pavers shaded with 13.4 °C, followed by the metal fence sunlit with 11 °C, the metal car

surface sunlit with 10.7 °C, the polished concrete floor shaded with 8.3 °C, the metal fence shaded with 7 °C, the asphalt road sunlit with 5.9 °C, the asbestos roofing sunlit with 5.3°C, the metal eaves sunlit with 4.8 °C, the light-colored block wall sunlit with 4.1 °C, the concrete pavers sunlit with 3.7 °C, and the smallest difference in the tree surface with 2 °C.

4.2. Section B

The surface temperatures of the urban street elements and building materials assessed in section B, considering the three points where the thermal images were taken, are presented in Table 3. Asphalt roads, concrete pavers, concrete sidewalk, block walls, concrete eaves, glass door, glass window, and metal car surface are the urban elements analyzed in this canyon.

Table 3. Surface temperatures of the street elements and building materials in section B.

	Visual Image	Thermal Image Aug.	Thermal Image Jan.	
4-5				
5-4				
5-6				
6-5				
	Spot	Surface	Temperature (°C) Aug.	Temperature (°C) Jan.
4-5	1	Concrete pavers sunlit	52.1	38.0
	2	Concrete pavers shaded	34.4	23.5
	3	Concrete sidewalk sunlit	50.7	35.5
	4	Concrete sidewalk shaded	31.9	24.8
	5	Metal car surface shaded	35.2	28.7
	6	Metal car surface sunlit	43.6	62.2
5-4	1	Asphalt road sunlit	41.2	27.0
	2	Asphalt road shaded	33.3	25.1
	3	Concrete eaves shaded	37.1	27.6
	4	Light-colored block wall shaded	33.5	27.2
	5	Dark metal car surface shaded	48.9	28.2
5-6	1	Asphalt road sunlit	44.1	28.3
	2	Asphalt road shaded	34.8	24.2
	3	Dark-colored block wall shaded	37.0	27.7
	4	Light-colored block wall shaded	31.3	24.4
	5	Glass window shaded	37.4	26.3
6-5	1	Asphalt road sunlit	43.6	29.2
	2	Asphalt road shaded	32.9	23.4
	3	Concrete eaves shaded	33.9	24.7
	4	Light-colored block wall sunlit	31.0	28.1
	5	Light-colored block wall shaded	31.2	24.2
	6	Glass door shaded	32.2	26.0

Surface temperatures in sunlit and shaded conditions during the warmest period are shown in **Figure 7(A)**. Due to climate conditions and urban form, most of the materials were studied in shaded conditions, except for the asphalt road, concrete pavers, concrete sidewalk, light-colored block wall, and metal car surface, which were analyzed in both conditions. Analyzing the surface temperature under sunlit conditions, concrete pavers, concrete sidewalk, metal car surface, and asphalt road show surface temperatures above 40 °C, with two of them even exceeding 50 °C. Only the light-colored block wall has a surface temperature near 30 °C under sunlit conditions. Meanwhile, during shaded conditions, all materials maintained a surface temperature between 30 °C and 40 °C, with the glass window and dark-colored block wall being the ones with the highest surface temperature, at 37.4 °C and 37 °C, respectively, while the concrete sidewalk presented the lowest, at 31.9 °C. Similar findings observed in Indonesia and Korea indicated that exposed glass windows obtained high surface temperatures ^[19,20], as well as dark-colored building facades ^[18,19]. Comparing the average differences in surface temperatures between sunlit and shaded conditions, the concrete sidewalk has a difference of 18.8 °C, the concrete pavers of 17.7 °C, the asphalt road of 8.8 °C, and the metal car surface of 8.4 °C.

While assessing the surface temperature during the coldest period [Figure 7(B)], the same pattern is replicated, but all the average surface temperatures of the urban elements and building materials during sunlit conditions are below 40 °C, except for the metal surface car, which reached 62.2 °C because it was a dark-colored car. In the shaded condition, all the materials have average surface temperatures between 20 °C and 30 °C. The average differences in surface temperatures between the concrete pavers in sunlit and shaded conditions show a difference of 14.5°C, and the concrete sidewalk of 10.7 °C.

The average surface temperatures between the warmest and coldest periods of the urban elements and building materials are presented in **Figure 7(C)**. All materials during the warmest period show higher average surface temperatures than during the coldest period, except for the metal car surface. Average surface temperatures during the warmest period are generally between 30 °C and 50 °C, while in the coldest period they are generally between 20 °C and 40 °C. The most significant differences in average surface temperature occur on the metal car surface sunlit with 18.6 °C, concrete sidewalk sunlit with 15.2 °C, asphalt road sunlit with 14.6 °C, concrete pavers sunlit with 14.1 °C, glass window shaded with 11.1 °C, and concrete pavers shaded with 10.9 °C.

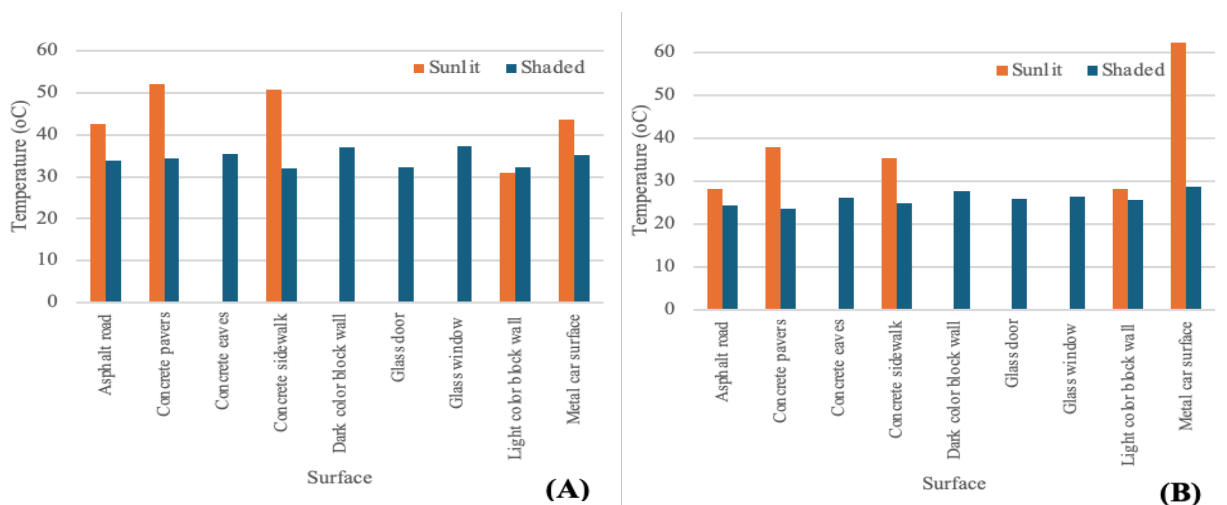


Figure 7. Cont.

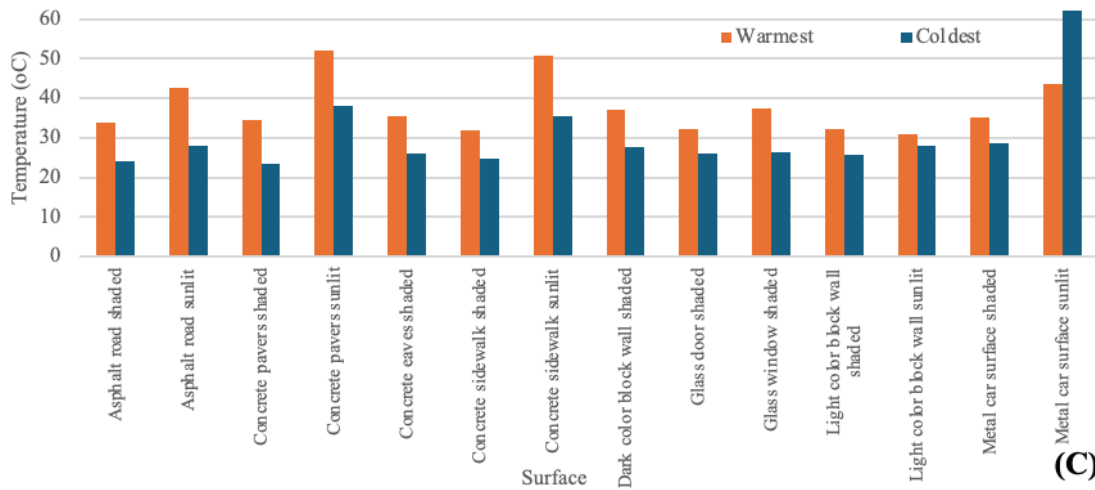


Figure 7. Surface temperature of the urban elements and building materials in Section B, (A) warmest period with sunlit and shaded, (B) coldest period with sunlit and shaded, and (C) both periods warmest-coldest.

4.3. Section C

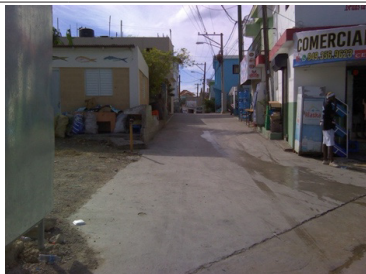

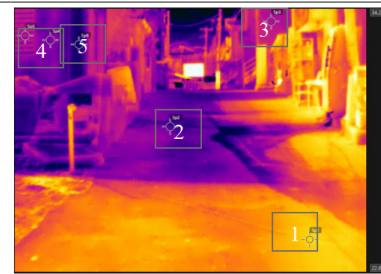


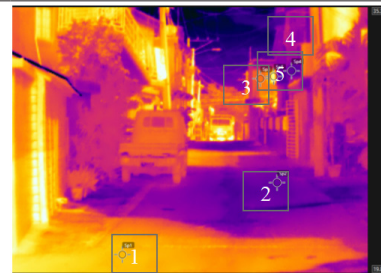
Table 4 shows the surface temperatures of the urban street elements and building materials studied in section C, considering the two points where the thermal images were taken. The urban elements analyzed in this canyon are asphalt roads, block walls, and glass windows.

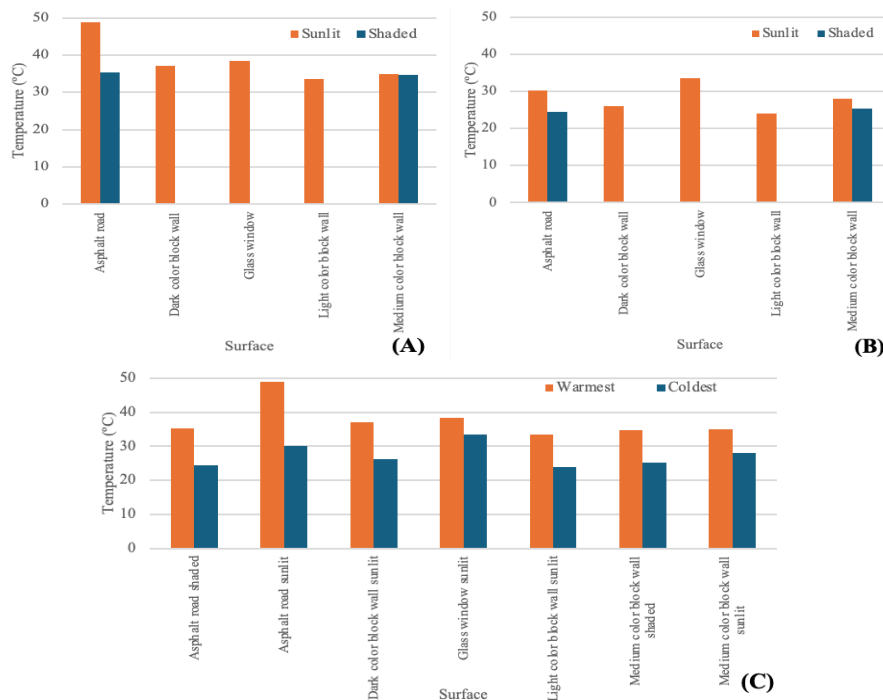
In this street canyon, most of the urban elements and building materials were studied in sunlit conditions, and only two materials, asphalt road and medium-colored block wall, were studied in both sunlit and shaded conditions. **Figure 8(A)** presents surface temperatures during the warmest period in sunlit and shaded conditions. All urban elements and building materials average surface temperatures under sunlit conditions are above 30 °C. The asphalt road had the highest average surface temperature under sunlit conditions with 48.9 °C, while the lowest average surface temperature was for the light-colored block wall with 33.6 °C. Meanwhile, under shading conditions, the asphalt road and medium-colored block wall have surface temperatures near 30 °C. Comparing the average differences in surface temperatures between the asphalt road in sunlit and shaded conditions shows a difference of 13.7 °C, and the medium-colored block

wall of 0.2 °C. This same pattern is repeated during the coldest period [**Figure 8(B)**], but all average surface temperatures of the urban elements during sunlit conditions are below 30 °C except for the glass window, which reached 33.5 °C. In this case, the average differences in surface temperatures between the asphalt road in sunlit and shaded conditions present a difference of 5.8 °C, and the medium-colored block wall of 2.7 °C.

Analyzing the average surface temperature between the warmest and coldest periods, all urban elements and building materials reported higher average surface temperatures during the warmest period compared to the average surface temperatures of the coldest period [**Figure 8(C)**]. The largest average surface temperature difference occurs in the asphalt road sunlit with 18.8 °C, followed by the dark-colored block wall sunlit with 11 °C, the asphalt road shaded with 10.9 °C, the light-colored block wall sunlit with 9.6 °C, the medium-colored block wall shaded with 9.4 °C, the medium-colored block wall sunlit with 6.9 °C, and the smallest difference in the glass window sunlit with 4.9 °C. Similar results were confirmed when the asphalt road has a strong influence, as it is constantly exposed to the sun, storing heat all day long, presenting high surface temperatures ^[1–19].

Table 4. Surface temperatures of the street elements and building materials in section C.

	Visual Image	Thermal Image Aug.	Thermal Image Jan.	
7-8				
8-7				
	Spot	Surface	Temperature (°C) Aug.	Temperature (°C) Jan.
7-8	1	Asphalt road sunlit	50.5	30.2
	2	Asphalt road shaded	35.4	24.8
	3	Dark-colored block wall sunlit	37.1	26.1
	4	Medium-colored block wall shaded	34.7	25.3
	5	Light-colored block wall sunlit	34.2	24.1
8-7	1	Asphalt road sunlit	47.3	30.1
	2	Asphalt road shaded	35.1	24.0
	3	Medium-colored block wall sunlit	34.9	28.0
	4	Light-colored block wall sunlit	32.9	23.9
	5	Glass window sunlit	38.4	33.5


Figure 8. Surface temperature of the urban elements and building materials in Section C, (A) warmest period with sunlit and shaded, (B) coldest period with sunlit and shaded, and (C) both warmest-coldest periods.

4.4. Section D

The surface temperatures of the urban street elements and building materials evaluated in section D, considering the four points where the thermal images were taken, are presented in **Table 5**. Concrete pavers, concrete sidewalks, concrete roadside curb, concrete eaves, block walls, wooden wall, glass window, metal roof, tile roof, stone fence, metal louver window, and metal car surface are the urban elements analyzed in this canyon.

Surface temperatures in sunlit and shaded conditions during the warmest period are shown in **Figure 9(A)**. Due to the urban form of these street canyons and sun path, most of the urban elements and building materials were studied either in sunlit or shaded conditions; only two of them, concrete pavers and concrete sidewalk, were analyzed in both conditions. Under the sunlit condition, the average surface temperature of the materials ranged from 30 °C to 50 °C, with two exceptions: the dark-colored wooden wall, which reached 53.3 °C, and the metal roof, with 23.5 °C. In the latter case, the building was air-conditioned, losing the cold through the roof. Meanwhile,

during the shaded condition, all materials maintained an average surface temperature between 30 °C and 40 °C, presenting two exceptions: the concrete sidewalk with 42.5 °C and the glass window with 45.1 °C. Comparing the average differences in surface temperatures between sunlit and shaded conditions, the concrete pavers have a difference of 10.2 °C, and the concrete sidewalk has a difference of 1.2 °C. Similar findings were observed in a study in which shadows generated by green areas played an important role in reducing surface temperatures and the UHI effect ^[1,10,18,19], as well as urban textile shading can provide a heat mitigation efficacy ^[17]. Additionally, Rodríguez et al. ^[16] observed that the lowest temperatures were observed in the tree canopy, remaining close to the air temperature throughout the day. Also, Tan et al. ^[35] indicated that green areas can shade the surfaces, preventing them from absorbing short-wave radiation, and they contribute to obtaining a fresher environment by converting sensible heat into latent heat through evapotranspiration of their leaves, having a lower albedo and a lower heat capacity than many artificial materials.

Table 5. Surface temperatures of the street elements and building materials in section D.

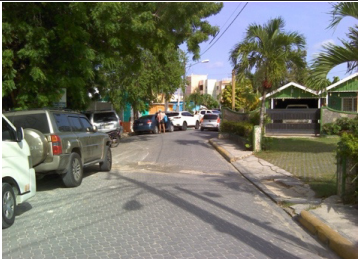



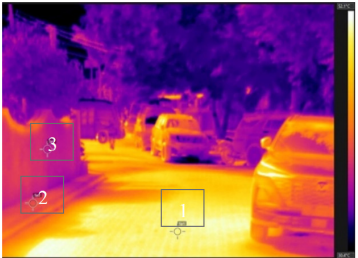





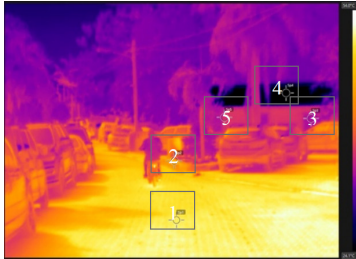







	Visual Image	Thermal Image Aug.	Thermal Image Jan.
9-10			
10-9			
10-11			

Table 5. Cont.

	Visual Image	Thermal Image Aug.	Thermal Image Jan.	
11-10				
11-12				
12-11				
	Spot	Surface	Temperature (°C) Aug.	Temperature (°C) Jan.
9-10	1	Concrete pavers sunlit	49.1	27.9
	2	Concrete pavers shaded	36.8	-
	3	Concrete sidewalk sunlit	43.7	-
	4	Concrete sidewalk shaded	44.8	26.9
	5	Metal car surface shaded	38.8	23.6
10-9	1	Concrete pavers sunlit	50.3	39.7
	2	Concrete sidewalk	40.2 (shaded)	38.5 (sunlit)
	3	Stone fence shaded	37.4	31.0
10-11	1	Concrete pavers sunlit	51.2	41.7
	2	Light-colored block wall sunlit	36.7	29.5
	3	Dark-colored wooden wall sunlit	53.3	-
	4	Tile roof sunlit	50.2	42.2
	5	Glass window shaded	45.1	-
11-10	1	Concrete pavers sunlit	50.7	38.7
	2	Concrete roadside curb sunlit	45.9	37.9
	3	Metal louver window	34.6 (shaded)	35.1 (sunlit)
	4	Metal roof sunlit	23.5	15.1
	5	Dark-colored block wall	37.0 (shaded)	50.3 (sunlit)
11-12	1	Concrete Pavers sunlit	47.7	37.5
	2	Medium-colored block wall sunlit	37.9	28.2
	3	Tile roof sunlit	48.4	38.6
	4	Light-colored block wall sunlit	36.2	27.7
12-11	1	Concrete pavers sunlit	50.9	35.0
	2	Concrete pavers shaded	41.7	24.5
	3	Dark-colored block wall shaded	40.5	29.0
	4	Dark-colored concrete eaves	44.5 (sunlit)	28.8 (shaded)
	5	Concrete roadside curb sunlit	40.0	36.3
	6	Stone fence	36.6 (shaded)	32.8 (sunlit)

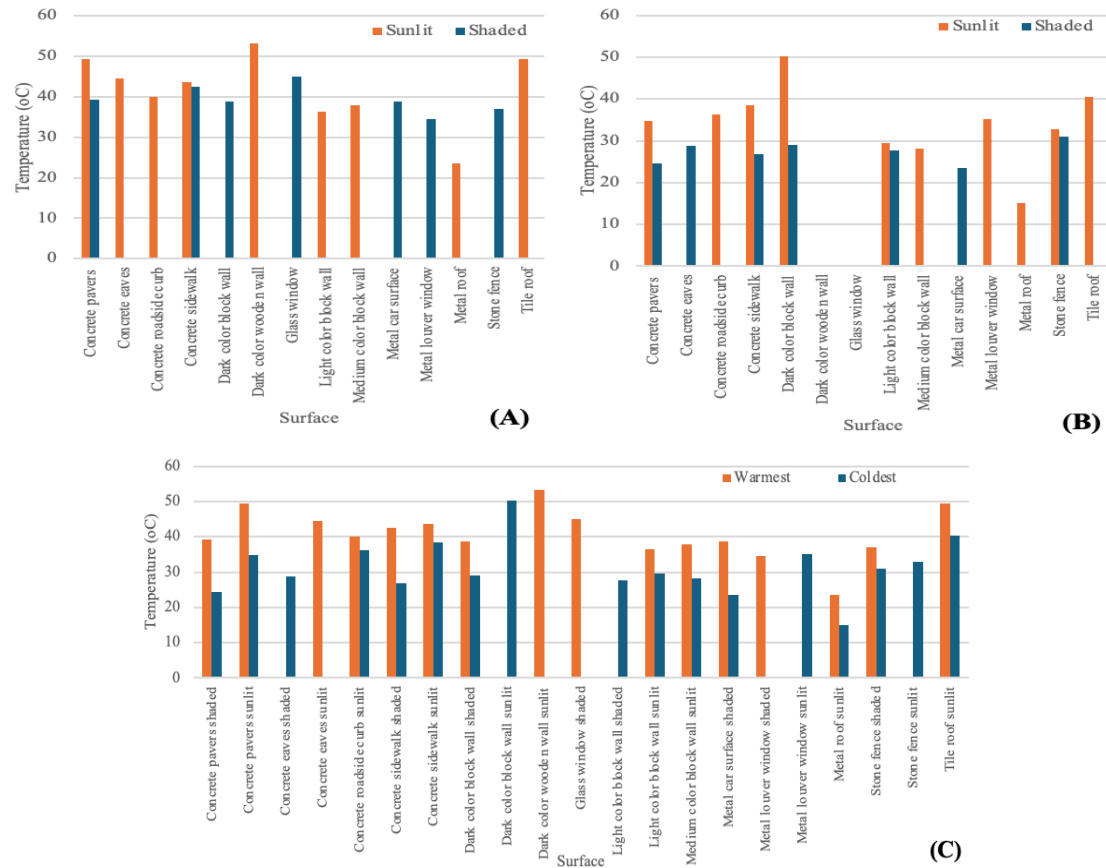


Figure 9. Surface temperature of the urban elements and building materials in Section D, (A) warmest period with sunlit and shaded, (B) coldest period with sunlit and shaded, and (C) both periods warmest-coldest.

Assessing the surface temperature during the coldest period [Figure 9(B)], the average surface temperatures of the urban elements and building materials during sunlit conditions are below 40 °C except for the dark-colored block wall, which reached 50.3 °C. In this case, the metal roof presents an average surface temperature of 15.1 °C due to the air-conditioning installed in the building. In the shaded condition, all the materials have average surface temperatures between 20 °C and 30°C, except for the stone fence, which reached 31 °C. The most important mean differences in surface temperatures under sunlit and shaded conditions were found in the dark-colored block wall with a difference of 21.3 °C, the concrete sidewalk with 11.6 °C, and the concrete pavers with 10.3 °C.

The mean surface temperatures between the warmest and coldest periods of the urban elements and building materials are presented in Figure 9(C). Most of the urban elements and building materials during the warmest period show higher average surface temperatures than during the coldest period. The average surface temperatures during

the warmest period are between 30 °C and 50 °C, and in the coldest period between 20 °C and 40 °C, except for the dark-colored wooden wall in both cases. The most significant differences in average surface temperature occur on the concrete sidewalk shaded with 15.6 °C, the metal car surface shaded with 15.2 °C, and the concrete pavers shaded and sunlit with 14.8 °C and 14.7 °C. Similar results from Indonesia agree that the high surface temperatures on the sloping surfaces of tile roofs may be caused by the higher solar radiation received and the high emissivity of this type of material ^[20].

4.5. Section E

Table 6 shows the surface temperatures of the urban street elements and building materials studied in section E, considering the two points where the thermal images were taken. The urban elements and building materials analyzed in this canyon are concrete pavers, concrete sidewalk, block walls, and glass windows.

Table 6. Surface temperatures of the street elements and building materials in section E.



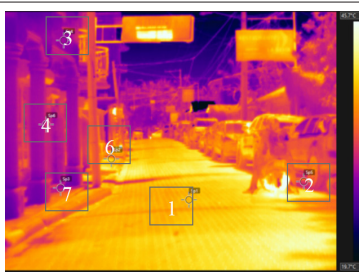



	Visual Image	Thermal Image Aug.	Thermal Image Jan.	
13-14				
14-13				
	Spot	Surface	Temperature (°C) Aug.	Temperature (°C) Jan.
13-14	1	Concrete pavers sunlit	36.9	38.8
	2	Concrete pavers shaded	33.8	32.7
	3	Light-colored block wall sunlit	31.2	29.9
	4	Medium-colored block wall sunlit	41.4	31.9
	5	Glass window sunlit	32.3	-
	6	Concrete sidewalk sunlit	39.7	39.5
	7	Concrete sidewalk shaded	36.0	30.1
14-13	1	Concrete pavers shaded	37.3	34.1
	2	Concrete sidewalk	36.6 (shaded)	37.4 (sunlit)
	3	Light-colored block wall sunlit	32.6	27.6

Figure 10(A) presents surface temperatures during the warmest period in sunlit and shaded conditions in the street canyon Section E. Most of the materials were studied in sunlit conditions, and only two materials, concrete pavers and concrete sidewalk, were studied in both sunlit and shaded conditions. Under sunlit conditions, all urban elements and building materials present average surface temperatures above 30 °C. The medium-colored block wall had the highest average surface temperature under sunlit conditions with 41.4 °C, while the lowest average surface temperature was for the light-colored block wall with 31.9 °C. Meanwhile, under shading conditions, concrete pavers and concrete sidewalk have surface temperatures of 35.6 °C and 36.3 °C, respectively. Comparing the average differences in surface temperatures between the concrete pavers in sunlit and shaded conditions shows a difference of 1.4°C, and the concrete sidewalk of 3.4 °C.

Figure 10(B) shows the surface temperature of the urban elements and building materials during the coldest period. In this case, the concrete pavers had the highest average surface temperature under sunlit conditions with

38.8 °C, while the lowest average surface temperature was for the light-colored block wall with 28.8 °C. Meanwhile, under shading conditions, concrete pavers and concrete sidewalk have surface temperatures of 33.4 °C and 30.1 °C, respectively. Comparing the average differences in surface temperatures between the concrete pavers in sunlit and shaded conditions shows a difference of 5.4 °C, and the concrete sidewalk shows a difference of 8.4 °C. Similar findings were observed in various studies in which concrete had a significant influence due to its heat storage capacity, resulting in high surface temperatures in all measured periods ^[1,15,16]. In addition, Tay et al. ^[36] indicated that concrete has long been the key element in achieving human thermal comfort in the tropical climate, as it constitutes one of the main components of many buildings.

Meanwhile, **Figure 10(C)** presents the average surface temperature between the warmest and coldest periods. Most of the urban elements and building materials reported higher average surface temperatures during the warmest period compared to the coldest period, except for the concrete pavers, which showed a slight difference

between the warmest and coldest periods. This is due to the time at which the thermal images were taken, having greater or lesser absorption of solar radiation during the daytime. The largest average surface temperature difference occurs in the medium-colored block wall sunlit with

9.5 °C, followed by concrete sidewalk shaded with 6.2 °C, light-colored block wall sunlit with 3.2 °C, concrete pavers shaded with 2.2 °C, concrete pavers sunlit with 1.9 °C, and the smallest difference in the concrete sidewalk sunlit with 1.3 °C.

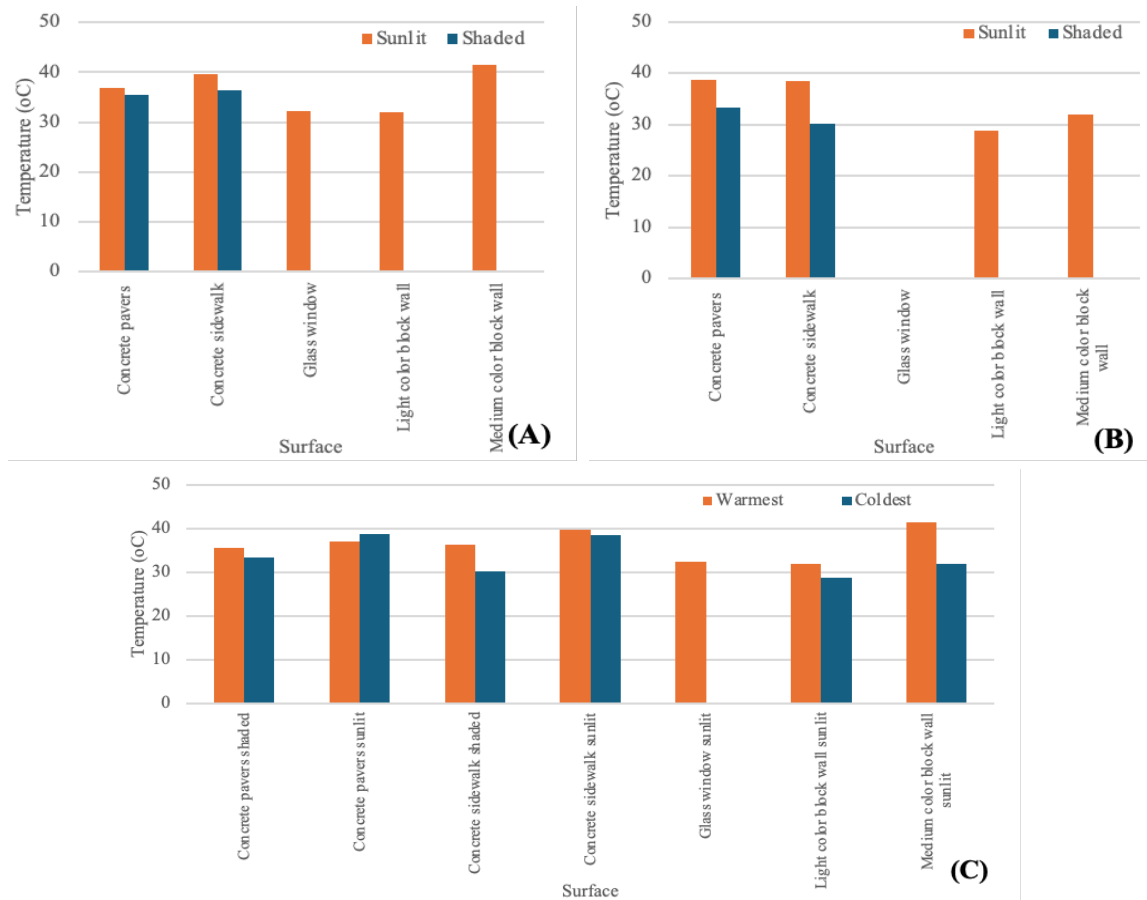


Figure 10. Surface temperature of the urban elements and building materials in Section E, (A) warmest period with sunlit and shaded, (B) coldest period with sunlit and shaded, and (C) both periods warmest-coldest

4.6. Section F

The surface temperatures of the urban street elements and building materials assessed in section F, considering the two points where the thermal images were taken, are presented in **Table 7**. Asphalt road, block walls, metal roof, and tile roof are the urban elements analyzed in this canyon.

Surface temperatures of the urban elements and building materials in sunlit and shaded conditions during the warmest period are shown in **Figure 11(A)**. Analyzing the surface temperature under sunlit conditions, most of the materials presented average surface temperatures between

30 °C and 50 °C, except for the tile roof, which presented 29.3 °C. Meanwhile, during shaded conditions, all materials maintained an average surface temperature between 30 °C and 40 °C, with the dark-colored block wall being the one with the highest temperature, at 35.6 °C, and the asphalt road being the lowest, at 31.4 °C. Comparing the average differences in surface temperatures between sunlit and shaded conditions, the dark-colored block wall has a difference of 14.2 °C, the asphalt road of 8.8 °C, the light-colored block wall of 2 °C, and the medium-colored block wall of 1.8 °C.





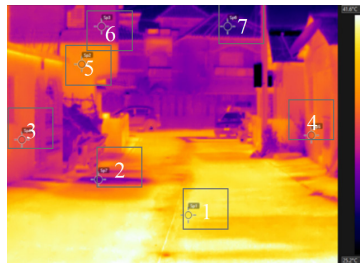

While assessing the surface temperature during the

coldest period [Figure 11(B)], the same pattern is observed, but all the average surface temperatures of the urban elements and building materials during sunlit conditions are below 40 °C, except for the metal roof, which reached 44.4 °C. In the shaded condition, all the materials have average surface temperatures between 25 °C and 30 °C. The average differences in surface temperatures between the asphalt road in sunlit and shaded conditions show a difference of 12.4 °C, the dark-colored block wall of 7.0 °C, and the medium-colored block wall of 6.3 °C.

Figure 11(C) presents the average surface temperatures between the warmest and coldest periods of the urban

elements. Most of the urban elements and building materials during the warmest period show higher average surface temperatures than during the coldest period, except for the metal roof, which is sunlit. During the warmest period, the average surface temperatures are generally between 30 °C and 50 °C, while in the coldest period they are generally between 20 °C and 40 °C, except for the metal roof. The most significant differences in average surface temperature occur on the dark-colored block wall, sunlit with 12.6 °C, and the metal roof, sunlit with 11.1 °C. The rest of the urban elements and building materials show differences of up to 6 °C.

Table 7. Surface temperatures of the street elements and building materials in section F.

	Visual Image	Thermal Image Aug.	Thermal Image Jan.	
15-16				
16-15				
	Spot	Surface	Temperature (°C) Aug.	Temperature (°C) Jan.
15-16	1	Asphalt road sunlit	40.5	34.9
	2	Asphalt road shaded	32.4	24.9
	3	Medium-colored block wall sunlit	36.4	35.0
	4	Metal roof sunlit	33.3	44.4
	5	Dark-colored block wall sunlit	49.7	31.7
	6	Light-colored block wall	34.3 (sunlit)	27.7 (shaded)
16-15	1	Asphalt road sunlit	39.8	41.0
	2	Asphalt road shaded	30.3	26.2
	3	Medium-colored block wall shaded	34.6	28.7
	4	Dark-colored block wall shaded	36.1	30.2
	5	Dark-colored block wall	35.0 (shaded)	42.6 (sunlit)
	6	Light-colored block wall shaded	32.3	28.6
	7	Tile roof sunlit	29.3	28.6

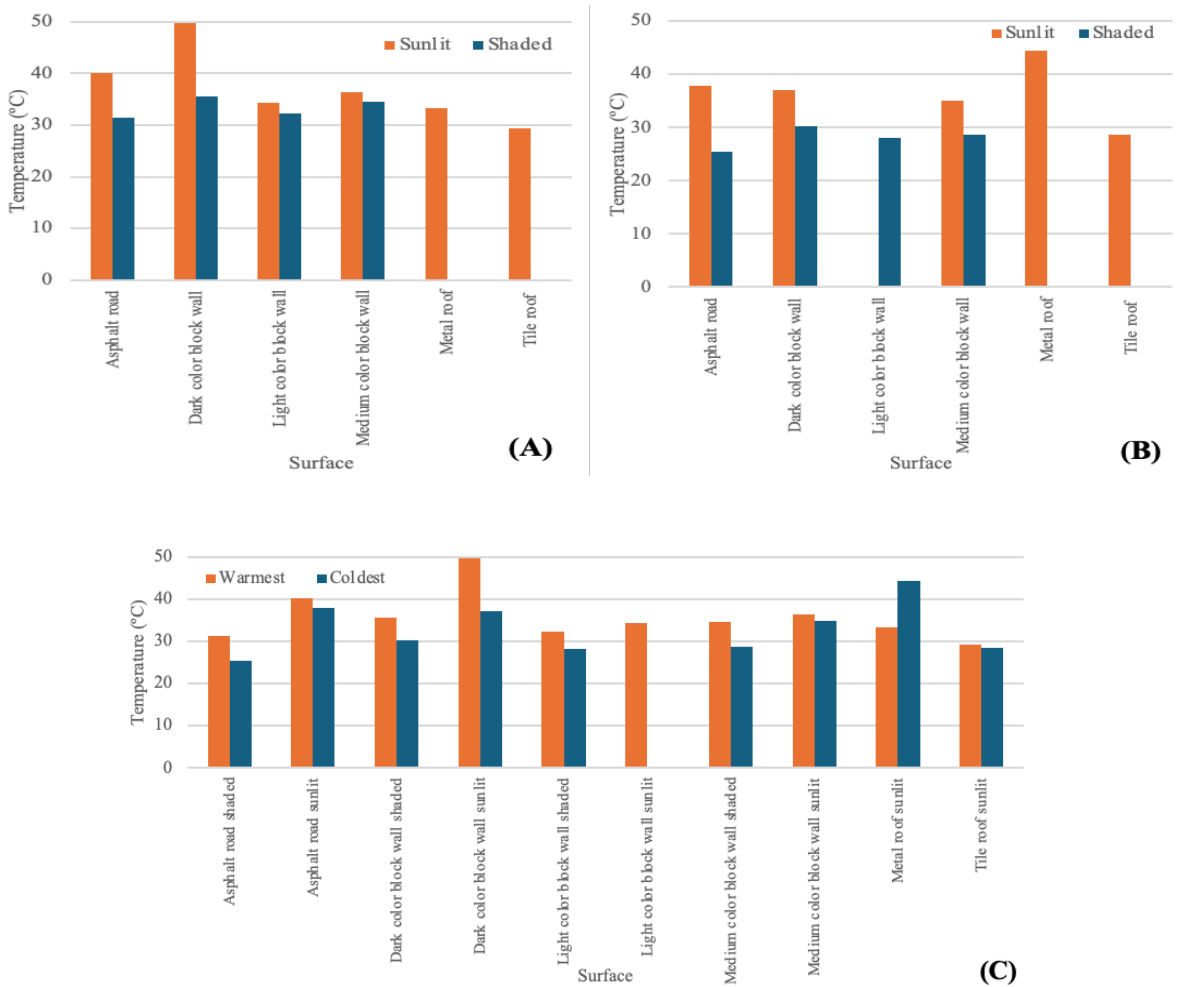


Figure 11. Surface temperature of the urban elements and building materials in Section F, (A) warmest period with sunlit and shaded, (B) coldest period with sunlit and shaded, and (C) both periods warmest-coldest

4.7. Surface Temperature Variability

Surface temperature variability between different urban street canyons is summarized in **Figure 12**. Most of the surface temperatures of urban elements and building materials are generally higher in the warmest period in all the urban canyons analyzed, while in the coldest period, the surface temperatures are lower, with some exceptions (e.g., dark-colored walls in sunlit). Analyzing the asphalt road, the highest surface temperatures occurred in the inner canyons C and F, with 48.9 °C in the warmest period and 37.9 °C in the coldest period, while in canyon B, with shade caused by vegetation in both periods analyzed, the lowest surface temperatures occurred, with 33.85 °C and

24.25 °C. Concerning concrete pavers in the conditions analyzed, the lowest surface temperatures were found in canyon E, located in front of the coast, and in the canyons that were shaded by vegetation (canyons B and D). The same behavior is present in the analyzed walls (e.g., light, medium, and dark colors), where the buildings located in front of the sea and shaded conditions presented lower surface temperatures than those located in interior canyons (e.g., canyons C and F). These results could be optimized by using computer vision to automatically segment infrared images by material type, shading conditions, and surface orientation, using robust and efficient vision-based models such as DeepLab^[37] and EfficientNet^[38].

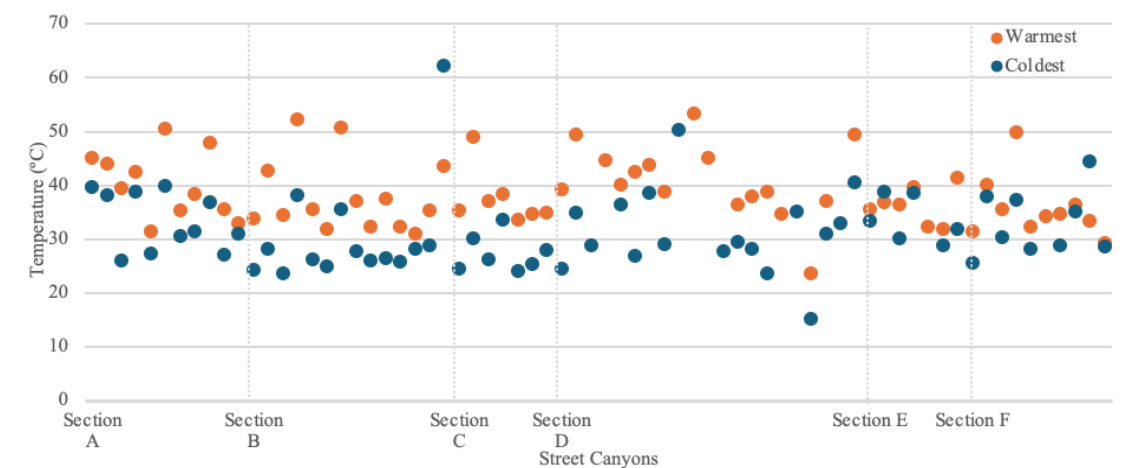


Figure 12. Surface temperature variability between different urban street canyons materials.

5. Conclusion

Using IRT, this research provides an analysis of six urban street canyons by evaluating surface temperatures of urban elements and building materials in the coastal city of Bayahibe, Dominican Republic. Thermal images were taken during the warmest and coldest weather conditions and distinguished between sunlit and shaded areas. The assessment allows the identification of the warmest and coldest areas of Bayahibe, providing a better understanding of the factors that influence the urban microclimate of the city under different meteorological conditions. The purpose of this research is to support strategies to mitigate the UHI effect and improve pedestrian thermal comfort in the context of a tropical climate.

Generally, sunlit surfaces of urban elements and building materials showed higher surface temperature readings compared to their shaded counterparts in both periods, warmest and coldest. The surface temperature of the materials in sunlit conditions can vary depending on factors such as the time of year, the angle of the sun, and the specific location of the canyon, such as one located in front of the coast or interior.

Metal car surfaces showed the greatest surface temperature difference, especially when comparing sunlit versus shaded conditions. The temperature of metal car surfaces varies widely depending on whether they are in direct sunlight or shade, as well as the color of the paint. Also, concrete pavers consistently showed higher temperatures when sunlit versus shaded. Asphalt roads exhibit the

same pattern, with sunlit areas being warmer than shaded areas. Block walls (light, medium, and dark colors) generally follow this trend as well. Light-colored block walls generally had lower surface temperatures in the warmest and coldest periods compared to medium and dark-colored block walls. This is because lighter colors reflect more sunlight, while darker colors absorb more heat, presenting higher temperatures.

Regarding the canyons, the lowest surface temperatures were found in those located in front of the coast and those with shade generated by the vegetation, while the canyons located in the interior of Bayahibe generally had the highest surface temperatures, directly affecting pedestrian comfort.

One limitation of this study is that the selection of the six canyons was not random, nor was it stratified according to known thermal factors (e.g., canyon aspect ratio), which could introduce selection bias and skew the apparent magnitude of the material effects. Also, the accuracy of the measurements presented in the paper may be affected by atmospheric attenuation effects due to the high humidity present in the environment. Additionally, some urban elements and building materials were only evaluated in sunlit or shaded conditions due to the urban form of the street and the orientation, which allowed or prevented the passage of solar rays. Therefore, it is recommended to perform the same thermal images on several days and at different times of the day to obtain data in all scenarios and to enable more comparisons between them. Further-

more, for thermal image processing and analysis, artificial vision could be used to enable accurate large-scale temperature mapping and reduce the bias of manual classification, using robust and efficient vision-based models such as DeepLab and EfficientNet. In addition, it would be very interesting to analyze the thermal role of vegetation by measuring the leaf water content, canopy density, and shading fraction, as vegetation represents an important shading element that affects the urban microclimate. Also, future work could incorporate full microclimatic modeling to link material surface temperatures with pedestrian thermal comfort using metrics like mean radiant temperature (MRT) or the Universal Thermal Climate Index (UTCI).

Overall, for tropical and coastal cities such as Bayahibe, the implementation of shading elements and the use of light colors contribute to maintaining a more comfortable urban microclimate for pedestrians than the use of medium and dark colors without solar protection, as well as contributing to the mitigation of the UHI effect. The results of this study can be used to develop specific interventions and policies aimed at creating more sustainable and climate-resilient urban environments in the Caribbean region.

Author Contributions

Conceptualization, L.R-V., V.F-S., V.W.B-L., and O.M-L.; methodology, L.R-V., V.F-S., V.W.B-L., and O.M-L.; formal analysis, L.R-V., V.F-S., and V.W.B-L.; writing—original draft preparation, L.R-V., V.F-S., V.W.B-L., and O.M-L.; writing—review and editing, L.R-V.; visualization, L.R-V., and V.F-S.; project administration, O.M-L.; funding acquisition, O.M-L. All authors have read and agreed to the published version of the manuscript.

Funding

This research is funding by project “Use of Digital Information Technologies for Adaptation of the Effects of Climate Change in Touristic Coastal Zones of the Dominican Republic” (ADAPT_CCDR), grant number FED/2020/420-874, funded by Harnessing Innovative Technologies to support Resilient Settlements on the Coastal Zones of the Caribbean (HIT RESET CARIBBE-

AN) implement by The University of the West Indies (The UWI), Anton de Kom University of Suriname (AdeKUS) and Caribbean Disaster and Emergency Management Agency (CDEMA), sponsored by the ACP-EU Innovation Fund, implemented by the Organization of African, Caribbean and Pacific States (OACPS) Research and Innovation Program, with the financial assistance of the European Union.

Institutional Review Board Statement

Not applicable.

Informed Consent Statement

Not applicable.

Data Availability Statement

Data is available upon request.

Conflicts of Interest

The authors declare no conflict of interest. The funders had no role in the design of the study; in the collection, analyses, or interpretation of data; in the writing of the manuscript; or in the decision to publish the results.

References

- [1] Elmarakby, E., Khalifa, M., Elshater, A., et al., 2022. Tailored Methods for Mapping Urban Heat Islands in Greater Cairo Region. *Ain Shams Engineering Journal*. 13(2), 101545. DOI: <https://doi.org/10.1016/j.asej.2021.06.030>
- [2] Di Napoli, C., Allen, T., Méndez-Lázaro, P.A., et al., 2023. Heat Stress in the Caribbean: Climatology, Drivers, and Trends of Human Biometeorology Indices. *International Journal of Climatology*. 43(1), 405–425. DOI: <https://doi.org/10.1002/joc.7774>
- [3] International Energy Agency, 2021. Key world energy statistics 2021. Available from: <https://www.iea.org/reports/key-world-energy-statistics-2021> (cited 22 March 2023).
- [4] Martin, M., Ramani, V., Miller, C., 2024. InfraRed Investigation in Singapore (IRIS) Observatory: Ur-

- ban Heat Island Contributors and Mitigators Analysis Using Neighborhood-Scale Thermal Imaging. *Energy and Buildings*. 307, 113973. DOI: <https://doi.org/10.1016/j.enbuild.2024.113973>
- [5] Al-Hafiz, B., 2017. Contribution to the Study of the Impact of Building Materials on the Urban Heat Island and the Energy Demand of Buildings [PhD Thesis]. Nantes, France: Université Bretagne Loire. pp. 1–295.
- [6] Klimenka, M., Zhao, K., Hilland, R., et al., 2025. Instant Infrared: Estimating Urban Surface Temperatures from Street View Imagery. *Building and Environment*. 267, 112122. DOI: <https://doi.org/10.1016/j.buildenv.2024.112122>
- [7] Martin, M., Chong, A., Biljecki, F., et al., 2022. Infrared Thermography in the Built Environment: A Multi-Scale Review. *Renewable and Sustainable Energy Reviews*. 165, 112540. DOI: <https://doi.org/10.1016/j.rser.2022.112540>
- [8] Tejedor, B., Lucchi, E., Nardi, I., 2022. Application of Qualitative and Quantitative Infrared Thermography at Urban Level: Potential and Limitations. In: Bienvenido-Huertas, D., Moyano-Campos, J. (eds.). *New Technologies in Building and Construction: Towards Sustainable Development*. Springer Nature, Singapore. pp. 3–19. DOI: https://doi.org/10.1007/978-981-19-1894-0_1
- [9] Ramani, V., Arjunan, P., Poolla, K., et al., 2024. Semantic Segmentation of Longitudinal Thermal Images for Identification of Hot and Cool Spots in Urban Areas. *Building and Environment*. 249, 111112. DOI: <https://doi.org/10.1016/j.buildenv.2023.111112>
- [10] Malcoti, M.D., Zia, H., Kabre, C., et al., 2023. Analysis of Urban Streets and Surface Thermal Characteristics Using Thermal Imaging Camera in Residential Streets of Gurugram City, India. *Environmental Science and Pollution Research*. 30, 86892–86910. DOI: <https://doi.org/10.1007/s11356-023-28553-2>
- [11] Martin, P., Baudouin, Y., Gachon, P., 2015. An Alternative Method to Characterize the Surface Urban Heat Island. *International Journal of Biometeorology*. 59, 849–861. DOI: <https://doi.org/10.1007/s00484-014-0902-9>
- [12] Quattrochi, D.A., Ridd, M.K., 1994. Measurement and Analysis of Thermal Energy Responses from Discrete Urban Surfaces Using Remote Sensing Data. *International Journal of Remote Sensing*. 15(10), 1991–2022. DOI: <https://doi.org/10.1080/01431169408954224>
- [13] Dorer, V., Allegrini, J., Orehounig, K., et al., 2013. Modelling the Urban Microclimate and Its Impact on the Energy Demand of Buildings and Building Clusters. *Proceedings of the 13th Conference of International Building Performance Simulation Association*; August 26–August 28, 2013; Chambéry, France. pp. 1176–1183. DOI: <https://doi.org/10.26868/25222708.2013.1176>
- [14] Kawakubo, S., Arata, S., Demizu, Y., et al., 2023. Visualization of Urban Roadway Surface Temperature by Applying Deep Learning to Infrared Images from Mobile Measurements. *Sustainable Cities and Society*. 99, 104991. DOI: <https://doi.org/10.1016/j.scs.2023.104991>
- [15] Rodriguez, M.V., Melgar, S.G., Marquez, J.M.A., 2023. Design Recommendations for the Rehabilitation of an Urban Canyon in a Subtropical Climate Region Using Aerial Thermography and Simulation Tools. *Energy and Buildings*. 298, 113525. DOI: <https://doi.org/10.1016/j.enbuild.2023.113525>
- [16] Rodríguez, M.V., Melgar, S.G., Márquez, J.M.A., 2022. Assessment of Aerial Thermography as a Method of In Situ Measurement of Radiant Heat Transfer in Urban Public Spaces. *Sustainable Cities and Society*. 87, 104228. DOI: <https://doi.org/10.1016/j.scs.2022.104228>
- [17] Garcia-Nevado, E., Beckers, B., Coch, H., 2020. Assessing the Cooling Effect of Urban Textile Shading Devices Through Time-Lapse Thermography. *Sustainable Cities and Society*. 63, 102458. DOI: <https://doi.org/10.1016/j.scs.2020.102458>
- [18] Lee, S., Moon, H., Choi, Y., et al., 2018. Analyzing Thermal Characteristics of Urban Streets Using a Thermal Imaging Camera: A Case Study on Commercial Streets in Seoul, Korea. *Sustainability*. 10(2), 519. DOI: <https://doi.org/10.3390/su10020519>
- [19] Febrita, Y., Hartono, R., 2023. Analysis of Thermal Characteristics of Urban Streets Using Thermal Imaging Camera: Case Study of Commercial Streets in Banjarbaru. *International Journal of Scientific Research in Science and Technology*. 10(6), 16–28. DOI: <https://doi.org/10.32628/ijrsr523105101>
- [20] Binarti, F., Pranowo, P., Leksono, S.B., 2020. Thermal Infrared Images to Identify the Contribution of Surface Materials to the Canopy Layer Heat Island in Hot-Humid Urban Areas. *Environmental and Climate Technologies*. 24(1), 604–623. DOI: <https://doi.org/10.2478/rtuct-2020-0037>
- [21] Belando, A.L., 2007. *La Romana and Bayahibe: Natural and Cultural Resources*. Amigo del Hogar: Santo Domingo, Dominican Republic. (in Spanish)
- [22] Rojas, V.T., 1993. *History of the Territorial Division (1492–1943)*. Editora Taller: Santo Domingo, Dominican Republic. (in Spanish)

- [23] Sistema de Inteligencia Turística (SITUR), 2025. La Romana 2025 Tourism Investment. Ministerio de Turismo: Santo Domingo, Dominican Republic. (in Spanish)
- [24] Dominican Republic (DO), 2025. Bayahibe. Available from: <https://www.godominicanrepublic.com/destinations/bayahibe/> (cited 17 February 2025).
- [25] Apple Inc., 2025. Maps. Map of the Town Bayahibe. Available from: <https://maps.apple.com/place?place-id=IBE11F0F9F9860A3&address=Camino+Playa+Bayah%C3%ADbe%2C+San+Rafael+Del+Yuma%2C+La+Altagracia%2C+Dominican+Republic&coordinate=18.37-27.47%2C-68.842108&name=Playa+Bayahibe&provider=9902> (cited 17 February 2025).
- [26] Izzo, M., Roskopf, C.M., Aucelli, P.P.C., et al., 2010. A New Climatic Map of the Dominican Republic Based on the Thornthwaite Classification. *Physical Geography*. 31(5), 455–472. DOI: <https://doi.org/10.2747/0272-3646.31.5.455>
- [27] Meteoblue, 2025. Simulated Historical Climate & Weather Data for Bayahibe. Available from: https://www.meteoblue.com/en/weather/historyclimate/climatemodelled/bayahibe_dominican-republic_3511624 (cited 17 February 2025).
- [28] Holiday-Weather, 2025. Bayahibe Live Weather. Available from: <https://www.holiday-weather.com/bayahibe/> (cited 17 February 2025).
- [29] Weather and Climate, 2025. Bayahibe, La Altagracia, Dominican Republic Climate. Available from: <https://weatherandclimate.com/dominican-republic/la-altagracia/bayahibe> (cited 17 February 2025).
- [30] Oficina Nacional de Estadística (ONE), 2024. General report of the 10th National Population and Housing Census 2022. Oficina Nacional de Estadística: Santo Domingo, Dominican Republic. pp. 62–93. (in Spanish)
- [31] Santana, E., n.d. Memories of Bayahibe. Available from: <https://www.facebook.com/groups/284652049129420> (cited 12 February 2025) (in Spanish)
- [32] Kylili, A., Fokaides, P.A., Christou, P., et al., 2014. Infrared Thermography (IRT) Applications for Building Diagnostics: A Review. *Applied Energy*. 134, 531–549. DOI: <https://doi.org/10.1016/j.apenergy.2014.08.005>
- [33] UNE-EN 13187, 1998. Thermal Performance of Buildings: Qualitative Detection of Thermal Irregularities in Building Envelopes. Infrared Method. Available from: <https://standards.iteh.ai/catalog/standards/sist/33adab5f-c195-46c3-b481-aa90963af87b/sist-en-13187-2000#:~:text=EN%2013187:1998%20%2D%20Thermal%20performance,01%2D-Nov%2D2023> (cited 25 March 2023).
- [34] ThermoWorks, 2024. Infrared Emissivity Table. Available from: <https://www.thermoworks.com/emissivity-table/?srsltid=AfmBOoq7XONBJLH6o-jiM8MisSpliWqTp73WRWDGOA0Wh5OMKzYKv-VB98> (cited 23 August 2024).
- [35] Tan, J.K.N., Belcher, R.N., Tan, H.T.W., et al., 2021. The Urban Heat Island Mitigation Potential of Vegetation Depends on Local Surface Type and Shade. *Urban Forestry & Urban Greening*. 62, 127128. DOI: <https://doi.org/10.1016/j.ufug.2021.127128>
- [36] Tay, L.T., Lee, Y.Y., Lee, Y.H., et al., 2022. A Review on the Behaviour, Properties and Favourable Characteristics for Thermally Insulated Concrete for Tropical Climate. *Journal of Engineering Science and Technology*. 17(3), 1608–1643.
- [37] Song, Z., Zou, S., Zhou, W., et al., 2020. Clinically Applicable Histopathological Diagnosis System for Gastric Cancer Detection Using Deep Learning. *Nature Communications*. 11, 4294. DOI: <https://doi.org/10.1038/s41467-020-18147-8>
- [38] Kabir, H., Wu, J., Dahal, S., et al., 2024. Automated Estimation of Cementitious Sorptivity via Computer Vision. *Nature Communications*. 15, 9935. DOI: <https://doi.org/10.1038/s41467-024-53993-w>